Longitudinal Solid Polarized Target for CLAS12

P. Pandey, S. Kuhn, V. Lagerquist, C. Keith, J. Brock, and J. Maxwell

Journal of Nepal Physical Society
Volume 8, No 2, 2022
(Special Issue: ANPA Conference 2022)
ISSN: 2392-473X (Print), 2738-9537 (Online)

Editors:
Dr. Pashupati Dhakal, Editor-in-Chief
Jefferson Lab, VA, USA
Dr. Nabin Malakar
Worcester State University, MA, USA
Dr. Chandra Mani Adhikari
Fayetteville State University, NC, USA

Managing Editor:
Dr. Binod Adhikari
St. Xavier's College, Kathmandu, Nepal

JNPS, **8** (2), 23-30 (2022)
DOI: http://doi.org/10.3126/jnphyssoc.v8i2.50144

Published by: Nepal Physical Society
P.O. Box: 2934
Tri-Chandra Campus
Kathmandu, Nepal
Email: nps.editor@gmail.com

ANPA Conference 2022
ISSN : 2392-473X(Print), 2738-9537 (Online)
Research Article ©Nepal Physical Society
DOI:http://doi.org/10.3126/jnphyssoc.v8i2.50144

Longitudinal Solid Polarized Target for CLAS12

P. Pandey,[1, a)] S. Kuhn,[1] V. Lagerquist,[1] C. Keith,[2] J. Brock,[2] and J. Maxwell[2]

[1)] *Old Dominion University, Norfolk, Virginia 23529, USA*
[2)] *Thomas Jefferson National Accelerator Facility, Newport News, Virginia 23606, USA*

[a)] *Corresponding author: ppand002@odu.edu*

Abstract. The Run Group C suite of experiments measure multiple spin-dependent observables by scattering an 11 GeV electron beam from longitudinally polarized nucleon targets inside the CLAS12 spectrometer in Hall B at Jefferson Lab. The dynamically polarized target built for these experiments has been extensively tested by the JLab Target Group in the Experimental Equipment Lab using an auxiliary 5 T magnet. We report on the operational experience with the target, the benchmarks achieved so far (using various polarizable materials) as well as the complete target setup, experimental readiness, and its present status. Our results show that all target components work well and the project has started successfully with the first beam on June 11, 2022.

Received: 30 August 2022 ; **Accepted**: 21 September 2022 ; **Published**: 31 December 2022

Keywords: Spin, Scattering, Polarized target, Polarization, Nuclear Magnetic Resonance, Dynamic Nuclear Polarization

INTRODUCTION

Polarization observables are fundamental tools for understanding the nucleon structure. Data from the scattering of polarized electrons by polarized targets allows one to examine the target's strong-interaction spin structure. The polarized solid state target is an indispensable experimental tool to study single and double polarization observables. Single and double polarization measurements have been performed with a variety of different particles beams [1].

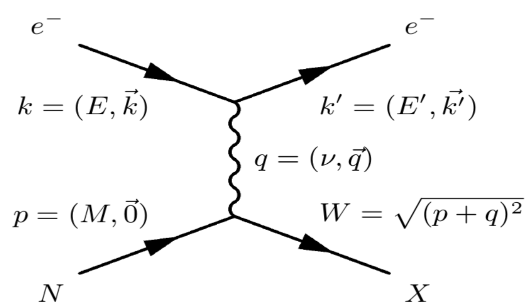

FIGURE 1. Feynman diagram for a eN scattering with single virtual photon exchange.

THEORETICAL BACKGROUND

Formalism

Because the interaction of the electron is well understood in terms of quantum-electrodynamics, the scattering of electrons can be used to probe unknown structure of hadronic systems. One of the best understood and effective ways of probing the internal structure of the nucleon is through lepton-nucleon scattering.

The electromagnetic interaction of a lepton with a nucleon is described by the exchange of virtual photons [2]. Figure1 shows the Feynman diagram of the scattering of a lepton off a nucleon in the one photon exchange. The incoming lepton with energy E and four momentum k scatters off a stationary target with mass M and four momentum 0, at an angle θ with energy E' and four momentum k'. On doing so, a virtual photon is exchanged whose four momentum is defined by the difference between that of the incident and the scattered lepton.

$$q = (p - p') = (\nu, \vec{q}). \tag{1}$$

The energy exchanged during the scattering process is

$$\nu = \frac{p.q}{M} = E - E'. \tag{2}$$

We define the squared four momentum transfer as

$$Q^2 = -q^2 \approx 4EE' sin^2 \frac{\theta}{2}, \tag{3}$$

which serves as a measure of the resolution power of the probing virtual photon. $Q^2 \to 0$ indicates the limit of scattering by a real photon, while $Q^2 \to \infty$ indicates the approach toward an infinitesimal distance resolution.
The Bjorken scaling variable, which is the momentum fraction of the struck parton is given as

$$x_B = \frac{Q^2}{2P.q}. \tag{4}$$

The scaling variable y is the fraction of the energy lost during the process,

$$y = \frac{p.q}{p.k} = \frac{\nu}{E}. \tag{5}$$

The invariant mass of the final unmeasured hadronic state is given as

$$W = \sqrt{(p+q)^2} = \sqrt{M^2 + 2M\nu - Q^2}. \tag{6}$$

Scattering regions

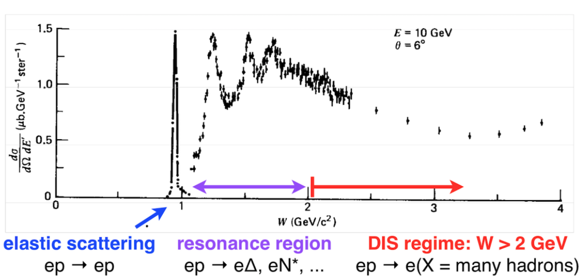

FIGURE 2. Differential cross section as a function of the invariant mass W [3].

Depending on the values of Q^2 and ν, the final state can emerge in different kinematic regions and can be distinguished in terms of the invariant mass (W) of the final state as shown in Fig. 2.

Elastic Scattering

Elastic scattering occurs when the target remains intact after the scattering. In other words, the final particles emerge without any structural modifications. Because the final state entity is simply the recoiling target, its invariant mass equals the target rest mass.

Resonances

When the energy transfer in the scattering process increases beyond the pion production threshold (when the combined invariant mass of the exchanged virtual photon and the target exceeds the value $W_\pi = M_p + M_\pi \approx 1.072$ GeV), we proceed towards the region of inelastic scattering, where we observe the rich spectrum of nucleon excitations known as resonances. These resonances show up as different isolated or overlapping peaks in the measured scattering cross sections. But since the resonances are short lived, these unstable particles promptly decay into other lighter particles. By studying polarized scattering in the resonance region, one can learn about internal structure of nucleon resonances and their excitations.

Deep Inelastic Scattering

On going to higher energy transfer ν and higher momentum transfer Q^2, the strengths of the resonances get weaker and at some point vanish. This region (also called the no resonance region), defined by $W > 2$ and $Q^2 > 1 - 2GeV^2$, is understood as a deep inelastic scattering (DIS) region. The virtual photon with sharp spatial resolution gets deep inside the nucleon and scatters off its constituents rather than from the whole target, which means the cross-section of scattering becomes the sum of cross-sections from different target constituents. The internal structure of the nucleons gets revealed. The target can fragment with additional particles produced in the final state. Polarization observables in this DIS region can reveal the spin carried by nuclear constituents (quarks and gluons).

SOLID POLARIZED TARGETS DESIGN AND GOALS

With Jefferson Lab's upgrade to a 12 GeV electron beam comes a new, improved detector system CLAS12 in Hall B. The new polarized target and its horizontal refrigerator fit in a space restricted by the new CLAS12 5 T solenoid and detector package, making the center of the target sit within a narrow clearance. The target dynamically polarizes NH_3 and ND_3 at 5 T and 1 K using 140 GHz microwaves, and hence provides polarized protons and deuterons. The various subsystems which comprise the target are the superconducting magnet, the 1 K refrigerator, the microwaves and nuclear magnetic resonance (NMR) systems, pumps, and the sample insert .
Figure 3 shows a simplified overview of these systems. The magnetic field is provided by superconducting coils and must achieve better than 10^4 uniformity in the region

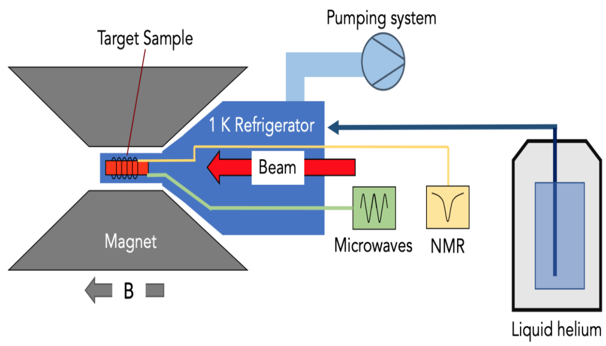

FIGURE 3. Simplified diagram of a DNP apparatus and its required systems.

of the target material to allow optimal polarizing conditions. The cryogenic temperatures are provided by a 1 K helium evaporation refrigerator which must accommodate the path of the incident beam and the scattered particles of interest in the detector system. Liquid helium is produced by JLab's End Station Refrigerator (ESR) and is continuously delivered to the Hall B "Buffer Dewar". The buffer Dewar has a volume of 500 liters and is automatically maintained at a liquid level of 70%.

The microwave frequency ($\sim$140 GHz) and power (1 W typical, up to 3 W) are monitored outside the cryostat and a multimode round waveguide transmits the microwaves inside the cryostat to a custom horn that distributes the power over the target. A continuous wave NMR system measures the target polarization.

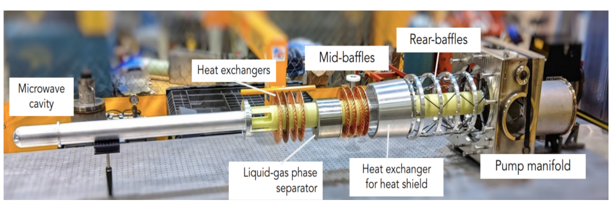

FIGURE 4. Refrigerator for polarized target experiment.

The cryostat is a 4.2 m long horizontal 1 K evaporation refrigerator designed and purpose built to fit inside the multilayered CLAS detector with several unique features. One design innovation is the method of target material replacement. This is required due to the accumulated radiation dose from the electron beam on the target which damages the target material and reduces the maximum achievable polarization. A novel mechanism, a retractable 1 K liquid helium bath (trolley) with swappable, preloaded sample cartridges (target cells), was developed in order to minimize the downtime required to change target material. This mechanism is contained inside a removal insert which serves as gliding rails for the 1 K bath trolley and supports the NMR and microwave components internal to the cryostat. This insert is nested inside the refrigerator and is easily removable when the refrigerator is warm. The surrounding refrigerator is supported by a modular, segmented truss structure, constructed from carbon fiber and glass- fiber-reinforced composite materials to minimize the thermal load as shown in Fig. 5. Radiation baffles are situated between each modular support followed by a conical heat exchanger that cools a surrounding thermal shield. All are cooled by exhausted helium gas from a 4 K liquid helium reservoir, the separator, that is fed from the buffer Dewar. Inside this reservoir is a porous metal mesh that separates the vapor boil off from the buffer Dewar transfer line and allows the incoming liquid helium to pass through and collect at the bottom of the reservoir as shown in Fig. 4. This stable volume of liquid helium supplies the refrigerator and prevents pressure oscillations from propagating through the rest of the system [4,5]. The liquid is siphoned from the separator, passing through the 1 K heat exchanger, to a miniature needle valve which both cools the liquid helium via the Joule-Thomson effect and controls the liquid level in the 1 K Bath.

1. Carbon Fiber Outer Vacuum Can
2. Al6062 Heat shield
3. Al7075 Pump Tube
4. Al6062 Shim Coil Mandrel
5. Cu:NbTi Multi-filament Superconducting Shim Coils
6. NMR/Trolley Insert

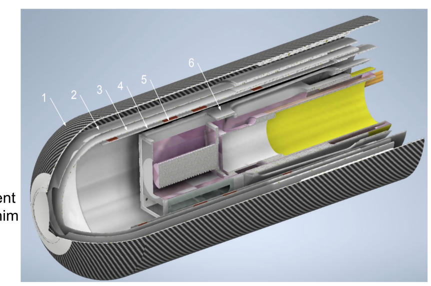

FIGURE 5. Different layers of refrigerator.

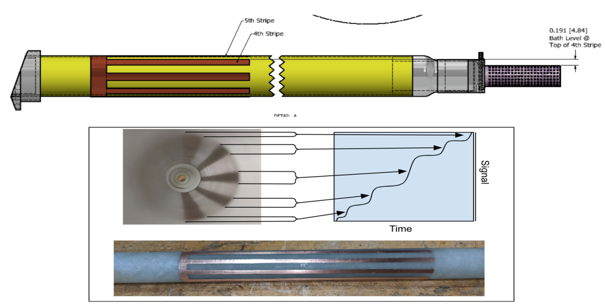

FIGURE 6. Level probe for helium level maintain.

A capacitive level probe, made of horizontal copper strips separated by a 1 mm gap, sits within the helium reservoir as shown in Fig.6. As the level increases, helium fills the gaps and changes the capacitance of the probe. The change is detected by an AC bridge circuit and lock-in amplifier, whose output controls the needle valve via a closed PID loop. In this manner, the level within the target bath can be maintained with sub-millimeter precision.

The aforementioned refrigerator components are internal to the helium pump tube that connects the 1 K Bath of liquid helium to a series of large Roots and rotary vane pumps. These lower the vapor pressure of the liquid, cooling it below 1 K (without additional heat loads e.g., microwaves, beam, etc.). This low temperature of the target material increases the spin-lattice relaxation time,T_1, of the protons or deuterons, and gives higher values of dynamic polarization.

The properties of a good polarized target material are a high number of polarizable nucleons compared to the total amount of nucleons (high dilution factor), high polarization degree, short polarization build up time, good resistance against radiation damage and easy handling of the target material [6]. Ammonia freezes at 195.5 K, and can be crushed through a metal mesh to produce beads of convenient size, allowing maximal heat removal when the material is immersed in superfluid helium.

The electron beam is rastered over the face of the target sample in order to evenly distribute both heat and radiation damage throughout the sample. While the maximum achievable polarization falls as continued radiation dose is accumulated, the damage can be partially repaired by annealing the sample in liquid argon for times ranging from a few minutes to several days.

For all parts of the RG-C experiments, we have 5 cm long cell, but they differ in their diameters. One type of

FIGURE 7. Upper: Pouring off the sample bottle sent from UVa, Lower: Loaded target cell in a proper cold LN2 bath.

cell is 15 mm in diameter whereas the other type is 20 mm. There are three different types of the target samples: polarized protons (NH_3), polarized deuterons (ND_3) and calibration targets (carbon, CH_2, CD_2, empty, etc).

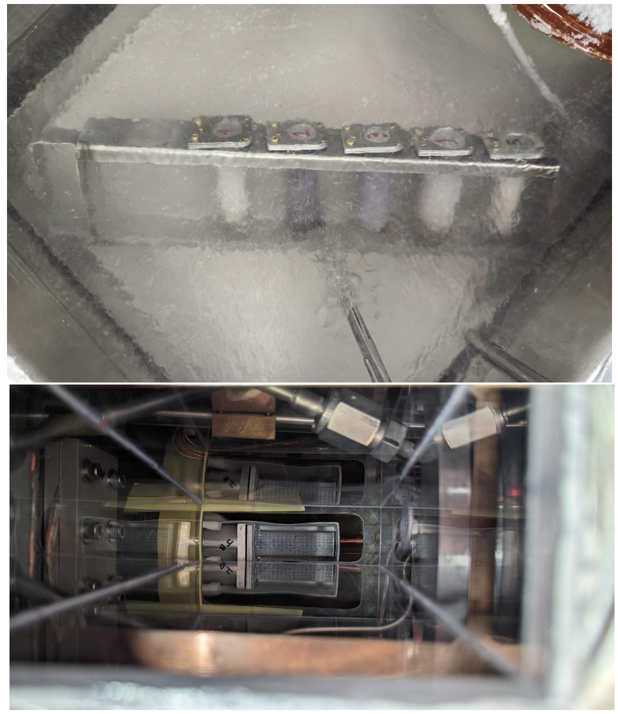

FIGURE 8. Top: Target cell placed in a ladder for storage, Bottom: Cell in a Teflon bath.

Target samples are loaded into small containers (cells) made of PCTFE (“Kel-F”) as shown in Fig. 7, and are securely placed in a storage container of liquid argon until needed. Cells are inserted into a small, rectangular bath made of Teflon inside the refrigerator as shown in Fig. 8. The bath is filled with liquid helium and cooled to 1 K prior to polarization.

METHOD OF POLARIZATION

Brute Force Polarization

A polarized target is an ensemble of particles placed in a high magnetic field and cooled to low temperature[7]. The Zeeman interaction between the external magnetic field B and the magnetic moment μ of the particles results in a set of $2I+1$ sublevels, where the spin $I=\frac{1}{2}$ is valid for protons and $I=1$ for deuterons.

The particles will have higher or lower energies based on if their magnetic moments are aligned or anti aligned. At large temperature and low magnetic field, the particles are pretty much equally distributed in higher and lower

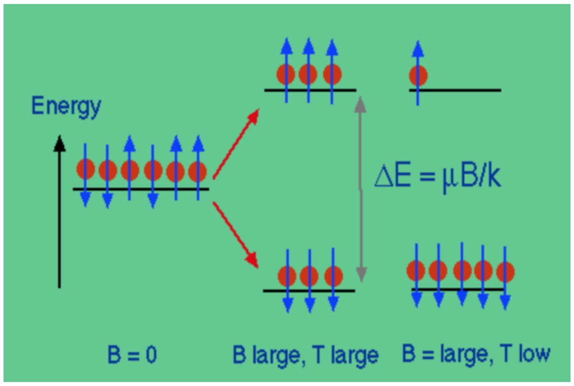

FIGURE 9. Thermal Equilibrium Polarization.

energy levels. But as we go on to really low temperature and high field, more particles with low energy fall into the lowest energy level as shown in Fig. 9. The populations of the energy levels are described by Boltzmann statistics. For the case of spin-1/2 particles,

$$\frac{n_-}{n_+} = e^{-\Delta E/kT} \tag{7}$$

where n_+ and n_- are the number of particles aligned and anti-aligned, T is the temperature of the system, ΔE is the Zeeman splitting of the two particle orientations, and k_B is Boltzmann's constant.

The polarization for the spin -$\frac{1}{2}$ system is given as

$$\begin{aligned} P(1/2) &= \frac{n_+ - n_-}{n_+ + n_-} \\ &= \tanh\left(\frac{\mu B}{k_B T}\right) \end{aligned} \tag{8}$$

and the vector polarization for the three-level spin-1 system is given as

$$\begin{aligned} P(1) &= \frac{n_+ - n_-}{n_+ + n_0 + n_-} \\ &= \frac{4\tanh\left(\frac{\mu B}{k_B T}\right)}{3 + \tanh^2\left(\frac{\mu B}{k_B T}\right)} \end{aligned} \tag{9}$$

Since the magnetic moment of the proton μ_p is small and that of the deuteron is even smaller, the nucleon polarization achieved with this method is very small. For 5T magnetic field and 1 K temperature, we can achieve only $\sim$ 0.5% polarization for protons and $\sim$ 0.1% for deuterons. These nucleon polarization values are not very useful for nuclear and particle physics experiments. However, electrons have higher magnetic moment ($\mu_e = 660\mu_p$) and are $\sim$ 99% polarized under the same conditions. Dynamic nuclear polarization leverages this fact to produce similarly high nuclear polarizations as shown in Fig. 10.

Dynamic Nuclear Polarization

In all experiments in order to measure the asymmetries, a strong net polarization must be induced in the target. The basic idea to obtain a high polarization of nuclear

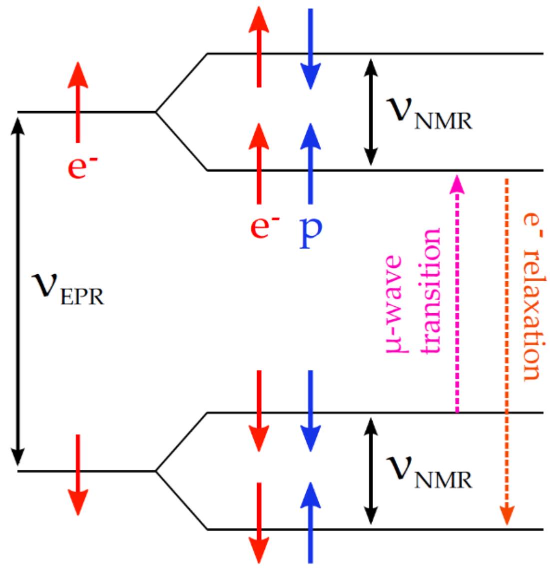

FIGURE 10. Dynamic Nuclear Polarization.

spins consists of using a microwave field, in a high magnetic field, to transfer the polarization of electron spins to these nuclei. In this technique, we first implant target material with paramagnetic impurities, polarize the electrons in these impurities via the brute force method previously described and use microwave irradiation to transfer the polarization of electrons to nuclei. Absorption of microwave radiation near the sum or difference of the electron and nuclear Larmor frequencies (ω_e and ω_n) produces simultaneous spin flips of both electrons and nuclei. If the microwave frequency is near $(\omega_e - \omega_n)$, nuclear spins in the upper Zeeman state will flip to a lower state, and a positive nuclear polarization will result. Microwaves near $(\omega_e + \omega_n)B$, cause nuclear spins in the lower state to flip to a higher state, leading to negative polarization. After a spin flip, the nuclear spin remains in its new energy level for several minutes or hours, while the electron spin returns to its lower energy level after only 100 ms or so and is thus available to polarize another nucleus. This is how we can get both negative and positive polarization as desired simply by adjusting the the microwave frequency.

NUCLEAR MAGNETIC RESONANCE

Continuous-wave Nuclear Magnetic Resonance (NMR) measures the target polarization. For this purpose, a re-designed "Q-meter" was developed at Jefferson Lab. The

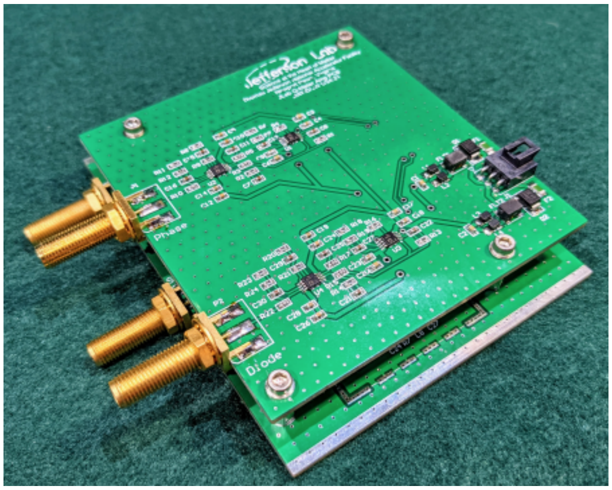

FIGURE 11. New JLab Q-meter.

new JLab Q-meter consists of 2 two-layer boards, ground-planed via stitching, see Fig. 11. It is enclosed in an Electromagnetic Interference (EMI) shielding enclosure. The

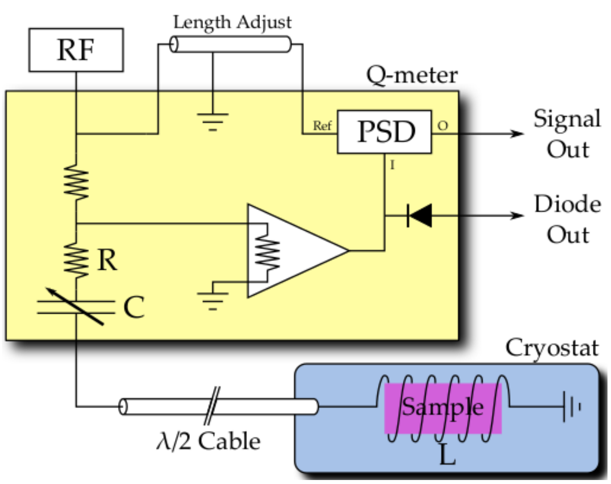

FIGURE 12. The yellow rectangle represents the actual Q-meter electronic box, while the blue shape represents the sample stick. RF is the NMR signal input.

Q meter is connected through a coaxial transmission cable to an NMR coil with inductance L that surrounds the target material, in series with a capacitance C and damping resistance R. Together, these form a series LCR circuit, see Fig. 12. NMR works by tuning the RLC circuit to the Larmor frequency of the desired nuclear spin. The Larmor frequency depends on the gyromagnetic ratio of the particle and on the external magnetic field. The Larmor frequency for the proton is very different to the deuteron, so two different RLC circuits are used.

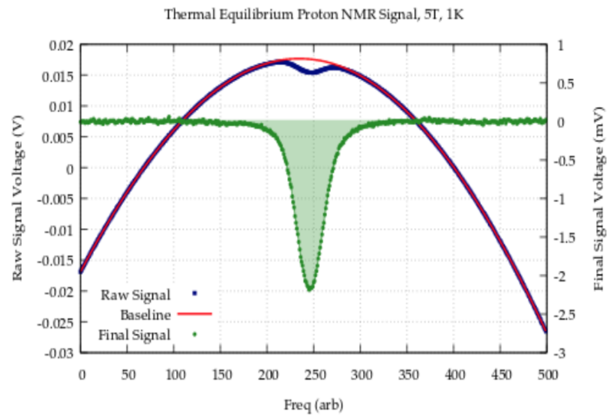

FIGURE 13. Proton TE signal at 5 T and 1 K, showing the raw Q-meter response in blue, a polynomial fit to the baseline in red, and the resulting NMR signal after subtraction in green.

The Q-meter measures the frequency response of the LCR circuit with the inductor embedded in the target material [9]. The RF frequency is swept through the proton (deuteron) Larmor frequency of 212.6 MHz (32.6 MHz). An RF field at the proton's Larmor frequency induces spin flips as the proton spin system absorbs or emits energy. By integrating the real portion of the response as the circuit is swept through frequency, a proportional measure of the sample's magnetic susceptibility, and thus polarization, is achieved. NMR "Q-curve" signals contain the frequency response of both the material's magnetic susceptibility, and the circuits' own background response. The baseline signal is recorded by lowering the magnetic field so that the NMR peak is shifted away from the frequency sweep range. Then we remove the background behavior of the NMR electronics to get the red baseline of the circuit which peaks at the resonant frequency as shown in Fig. 13. The baseline is subtracted and a polynomial fit to the wings of the resulting curve is performed, allowing the subtraction of any residual background shifts in the Q-curve. The degree of polarization is then proportional to the integrated area under this background-subtracted signal.

To determine the coefficient of proportionality, we measure the integrated signal area A_{TE} at a known polarization P_{TE} in a so-called "thermal equilibrium" measurement. An enhanced polarization can then be calculated from a signal area A during DNP by $P = A\left(\frac{P_{TE}}{A_{TE}}\right)$. A new online data analysis software data package has been written in Python to allow communication to the accelerator's EPICS control system and facilitate running, tuning, taking baselines, thermal equilibrium curve fits, and multilevel modular online data analysis with selectable fits.

Typical NMR signals for the proton and deuteron are displayed in Fig. 14, . The proton signal has only one peak and the deuteron signal has two peaks since it has three magnetic substates (-1, 0 and 1). The two spin transitions occurs between $-1 \rightarrow 0$ and $1 \rightarrow 0$. The deuteron vector polarization can be estimated using the relative heights of the two peaks.

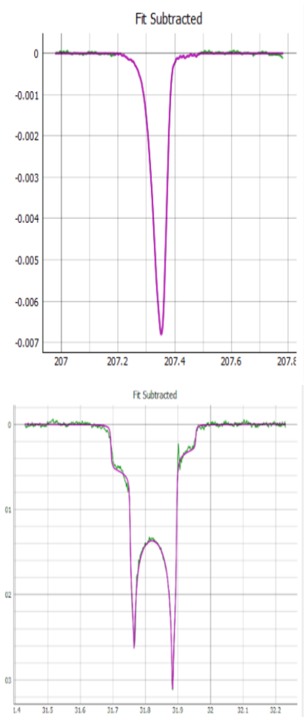

FIGURE 14. Top: positive proton signal with one peak, bottom: positive deuteron signal with 2 peaks.

$$P_d = \frac{r^2 - 1}{r^2 + r + 1}$$

where r is the ratio of the two transition peaks.

POLARIZED TARGET INSTALLATION

Run Group C experiments are scheduled to run from June 2022 to March 2023 and will be split between two configurations of the CLAS12 Forward Tagger (FT). The FT permits detection of electrons at smaller scattering angles but limits the rate of data acquisition. Approximately 25% of the allocated time will be spent with the FT in place (FT-in) and the remaining 75% with the FT removed (FT-out).

In May of 2022, the polarized target was successfully installed and incorporated into the CLAS12 detector of Hall B at Jefferson Lab as shown in Fig. 15. We got the first beam on June 11, 2022 and will run until March 14, 2023. The first part of the Forward Tagger ON configuration is completed. The change of the configuration took place during the last week of August, 2022. Since then, we have been running with forward tagger OFF configuration. We detect both the scattered electrons and leading hadrons from the hadronization of the struck quark[10]. With the RG-C suite of experiments, we aim to measure DIS inclusive spin structure functions of the proton and the deuteron, spin- and transverse momentum-dependent (TMD) parton distribution functions (PDFs) for Semi-inclusive Deep Inelastic Scattering (SIDIS), and target single and beam/target double spin asymmetries in proton and neutron Deeply Virtual Compton Scattering (DVCS). The target has produced proton and deuteron polarizations as high as 75% and 35%, respectively. We are cross-checking the target polarization values extracted using traditional NMR methods and from elastic scattering asymmetries.

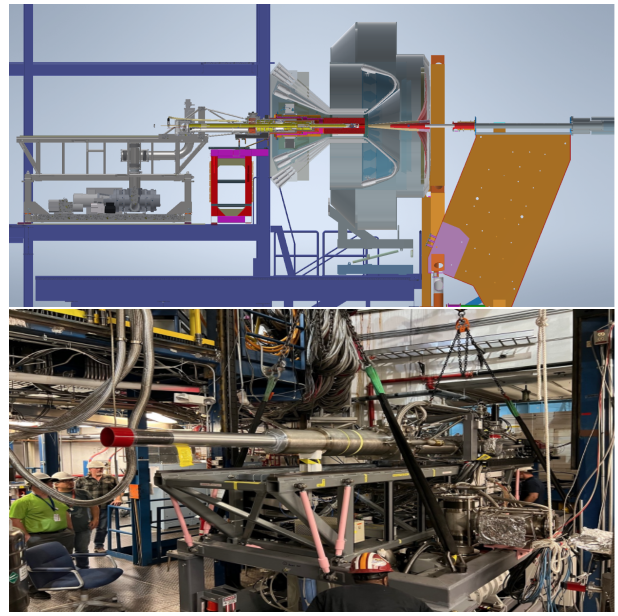

FIGURE 15. Target successfully installed in Hall B of Jefferson Lab for RG-C experiment.

CONCLUSIONS AND OUTLOOK

Here we reported on the design, construction, and performance of a polarized solid target for use in electron scattering experiments with the CEBAF Large Acceptance Spectrometer with the collaborative work of the polarized target groups at Jefferson Lab, University of Virginia (UVa), Christopher Newport University (CNU) and Old

Dominion University (ODU).

ACKNOWLEDGMENTS

We would like to thank our CLAS12 collaborators on Run Group C experiments for the opportunity to present our shared efforts. This work is supported by The U.S. Department of Energy (DOE), under contracts DE-AC05-06OR23177 (Jefferson Lab) and DE-FG02-96ER40960 (ODU).

EDITOR'S NOTE

This manuscript was submitted to the Association of Nepali Physicists in America (ANPA) Conference 2022 for publication in the special issue of Journal of Nepal Physical Society.

REFERENCES

1. S. Kuhn *et al.*, Spin structure of the nucleon—status and recent results, Progress in Particle and Nuclear Physics **63**,1–50 (2009).
2. R. G. Fersch *et al.*, Determination of the proton spin structure functions for $0.05 < Q^2 < 5GeV^2$ using CLAS, Phys. Rev. C **96**, 065208 (2017).
3. F. Halzen and A.D. Martin, An Introductory Course In Modern Particle Physics, *Wiley; 1st edition* (January 16, 1991)
4. J. Brock, Designs and construction techniques for the CLAS12 Dynamically Polarized Target, International Spin Symposium, Ferrara, Italy, September, 2018.
5. C. Keith *et al.*, A polarized target for the CLAS detector, Physics Research Section A **501**, 327 (2003).
6. W. Meyer, Ammonia as a polarized solid target material–a review, Nucl. Instrum. Methods Phys. Res. A **526** (1–2), 12 (2004).
7. D.G. Crabb and W. Meyer, Solid polarized targets for nuclear and particle physics experiments, Annual Review of Nuclearand Particle Science **47**, 67 (1997).
8. J. Maxwell, NMR Polarization Measurements for Jefferson Lab's in Proc. of Science, Volume 324 - XVII International Workshop on Polarized Sources, Targets Polarimetry (PSTP2017) - Polarized solid targets.
9. J. Maxwell *et al.*, Design and performance of the spin asymmetries of the nucleon experiment, Nuclear Instruments and Methods in Physics Research Section **885**, 145 (2018).
10. A CLAS Collaboration proposal, The Longitudinal Spin Structure of the Nucleons, A 12 GeV Research Proposal to Jefferson Lab (PAC 30).